JPEDAV (2010) 31:238–249
DOI: 10.1007/s11669-010-9695-7
1547-7037 ©ASM International

Thermodynamic Evaluation of the Si-C-Al-Y-O System for LPS-SiC Application

Zhu Pan, Olga Fabrichnaya, Hans J. Seifert, Roland Neher, Kristina Brandt, and Mathias Herrmann

(Submitted November 19, 2009; in revised form January 15, 2010)

A thermodynamic dataset for the Si-C-Al-Y-O system was developed for calculations of heterogeneous phase equilibria and reactions in SiC-base engineering ceramics. The quinary system is of major interest for the understanding of the liquid phase sintering of silicon carbide ceramics using additives like alumina (Al_2O_3) and yttria (Y_2O_3). The thermodynamic dataset was developed by the CALPHAD method of thermodynamic optimization. Analytical descriptions for the Gibbs free energy functions of all phases in the Si-C-Al-Y-O system were assessed. The sublattice model using the compound energy formalism was used for the treatment of the solid phases. The liquid phase was described by using the partially ionic liquid model presented as $(Al^{3+}, Si^{4+}, Y^{3+})_P(O^{2-}, SiO_4{}^{4-}, Va, AlO_{3/2}, SiO_2, C)_Q$, which covers metallic liquid and oxide liquid as a single phase.

Keywords LPS-SiC, phase diagram, Si-C-Al-Y-O system, thermodynamic modeling

1. Introduction

Silicon carbide (SiC) is one of the promising structural materials for mechanical and thermal applications because of its excellent properties, with regard to strength, hardness, chemical stability, wear and oxidation resistance, high thermal conductivity, creep and thermal shock.[1,2] It is also a promising inert matrix fuel material for irradiation of plutonium and minor actinides because of its irradiation damage tolerance.[3-6]

The sintering of SiC is usually performed at very high temperatures up to 2200 °C in the solid state (SSiC), with small amounts of boron, carbon, or aluminium as additives because of the strong Si-C bond and low self-diffusion coefficients. In the 1980s liquid phase sintered silicon carbide LPSSiC was developed as a material with higher fracture toughness than the SSiC but with a similar hardness. Sintering additives like Y_2O_3/Al_2O_3, AlN or other rare earths form a liquid phase at remarkably lower temperatures thus allowing a reduction of the sintering temperature. The additives crystallize during cooling and mostly form rare earth aluminates especially of garnet structure (YAG, $Y_3Al_5O_{12}$).[7-15]

The oxygen content of SiC powder, existing either as surface SiO_2 or as interstitial oxygen is between 0.8 and 1.1 wt.% SiO_2.[16-21] Surface SiO_2 is detrimental to the solid state sintering of SiC because gas evolution at the SiC/SiO_2 interface can cause the destruction of inter-particle connects and lead to excessive porosity in the final specimen.[21] Weight loss and microstructure development studies during liquid phase sintering with Al_2O_3-Y_2O_3 additives as well as thermodynamic calculations were performed by Grande et al.[16] It should be mentioned that, in the case of liquid phase sintering, surface SiO_2 can react with the sintering additives Al_2O_3 and Y_2O_3 and form an oxide liquid phase at even lower temperatures than the oxide liquid phase produced by reactions between Al_2O_3 and Y_2O_3 alone.[20] For example, although the lowest eutectic temperature in the Al_2O_3-SiO_2 pseudo-binary system is at 2083 K,[20] Mulla et al. reported liquid phase formation at about 2033 K[17] and Lee et al. showed sudden densification of SiC with Al_2O_3 and Y_2O_3 additives at 1773 K.[9] However, during liquid phase sintering SiO_2, Y_2O_3 and Al_2O_3 react with SiC resulting in gaseous CO, SiO, Al_2O and Al. These interactions cause weight losses, porosity and the formation of sintering skins or even instabilities of the materials.[22-28]

The understanding of the sintering and microstructure formation in these materials is the preposition of their reproducible production. Computational thermodynamics can support the understanding and modeling of reactions and process described above Ref 22, 26. The aim of present paper is to review available experimental and thermodynamic data for the relevant systems and to develop thermodynamic database for application of SiC liquid phase sintering.

2. Thermodynamic Data of the System

Several research groups contributed to derive thermodynamic parameters for the Y_2O_3-Al_2O_3-SiO_2 system. Fabrichnaya et al.[29] assessed the Y_2O_3-Al_2O_3-SiO_2 system and its subsystems based on available experimental phase diagrams and calorimetric measurements of solid phases. They described the liquid phase with the ionic two-sublattice model using the formula $(Y^{3+})_P(O^{2-}, SiO_4{}^{4-}, AlO_{1.5}, SiO_2)_Q$. Later Mao et al.[30] re-assessed thermodynamic properties in the

Zhu Pan, Olga Fabrichnaya, and **Hans J. Seifert**, Institute of Materials Science, Technical University of Freiberg, 09599 Freiberg, Germany; **Roland Neher, Kristina Brandt,** and **Mathias Herrmann**, Fraunhofer Institute for Ceramic Technologies and Systems, 01277 Dresden, Germany. Contact e-mail: zhupan@ww.tu-freiberg.de.

Y_2O_3-Al_2O_3-SiO_2 ternary system and its constituent binaries Y_2O_3-Al_2O_3 and Y_2O_3-SiO_2 using different species in the model of ionic liquid than Fabrichnaya et al.[29] The liquid phase was described by the ionic two-sublattice model with the formula $(Al^{3+}, Y^{3+})_P(AlO_2^{1-}, O^{2-}, SiO_4^{4-}, SiO_2^0)_Q$. With this model, the liquid miscibility gap in the SiO_2 rich part of ternary system can be reproduced better than in the work of Fabrichnaya et al.[29] However, the deviations from experimental data for invariant reactions were large in work of Mao et al.[30] (see Table 1). Mao et al.[30] considered two versions of database. According to calculations with dataset-1, which the authors[30] gave some preference, the $Y_2Si_2O_7$ phase in Y_2O_3-SiO_2 binary system melts congruently contradicting experimental data. For the description of liquid phase sintering, the SiO_2-rich part of phase diagram is not very important, because silica content on SiC surface does not exceed 2 mass%. Based on this consideration, the dataset of Fabrichnaya et al.[29] was accepted as the starting point in this work for further re-assessment using the same thermodynamic models for phases as in Fabrichnaya et al.[29] Additionally, the comparison of results for the Si_3N_4-AlN-Al_2O_3-SiO_2 system obtained by Dumitrescu and Sundman[31] with recent assessment of Mao et al.[32] did not reveal any advantage of using ionic liquid model with AlO_2^{1-} species.

Thermodynamic database for the Y_2O_3-Al_2O_3-SiO_2 system of Ref 29 was incorporated into the database for the Al-C-O-Si-Y system[33] by Cupid et al.[34] Calculations were performed by Cupid et al.[34] to explore some aspects of the thermodynamics of liquid phase sintering of SiC with Al_2O_3 and Y_2O_3 additives. However, in the work of Cupid et al.[34] two different descriptions of liquid were used, for metallic liquid and ionic oxide liquid. In the Y-O rich compositions, such simplification cannot be accepted, because in the Y-O system the liquid phase continuously dissolves oxygen and certainly does not decompose into two liquid phases.

Recently, the thermodynamic description of yttrium was updated and recommended by the Scientific Group Thermodata Europe.[35]

Therefore, the aim of this work was the development of a self-consistent thermodynamic database for the Al-Si-Y-C-O system which can be used for modelling of liquid phase sintering of SiC. All systems including yttrium should be updated, checked for consistency with experimental data and re-assessed if necessary. Two-sublattice partially ionic liquid model describing the liquid phase in wide composition ranges from metallic liquid to oxide ionic liquid and finally to highly polymerized SiO_2 liquid should be incorporated.

3. Thermodynamic Modeling

The CALPHAD (CALculation of PHAse Diagrams) method[36,37] was used to determine phase equilibria and phase reactions in the multi-component systems. Unary data for the pure elements[38] and descriptions of gaseous species were taken from the SGTE substance database.[35] Thermodynamic description of Al-C, Al-O, Al-Si, C-Si, C-O and Si-O binary systems were taken from SGTE database (SSOL, solution database and SSUB, substance database see Ref 35). The Al-Y,[39] C-Y[40] and Si-Y[41] systems were updated by Lukas using new pure yttrium SGTE-data for publication in Landoldt-Börnstein series. These results were also adopted in present work. Recently new thermodynamic

Table 1 Invariant phase equilibria including the liquid phase in the Y_2O_3-Al_2O_3-SiO_2 system

Solid phases in equilibrium with the liquid phase	Comparison of equilibrium conditions between experiments and assessments		
		Liquid composition, mass%	
	Temperature, K	Al_2O_3	SiO_2
$Y_2O_3R + Y_2SiO_5 + YAM$	2113(a)	8.5(a)	11.0(a)
	(2018) <2060> {2031}	(4.7) <5.4> {8.8}	(10.2) <8.6> {9.3}
Mul + Tri + $\gamma - Y_2Si_2O_7$	1618(a), 1644(b)	22.0(a), 25.1(b)	46.0(a), 44.2(b)
	(1558) <1620> {1625}	(20.3) <20.6> {21.7}	(47.7) <54.8> {47.6}
Y_2SiO_5 + YAM + YAG	(1961) <2018> {1908}	(16.9) <20.1> {21.1}	(12.6) <10.0> {11.6}
YAM + YAP + YAG	(1966) <2020> {1919}	(16.9) <20.2> {21.3}	(12.4) <9.8> {10.8}
Mul + Al_2O_3 + $\gamma - Y_2Si_2O_7$	(1630) <1715> {1685}	(24.5) <24.4> {24.0}	(33.5) <40.0> {38.2}
Y_2SiO_5 + YAG + $\gamma - Y_2Si_2O_7$	(1706) <1851> {1737}	(20.9) <36.1> {24.1}	(24.1) <20.8> {24.0}
YAG + Al_2O_3 + $\gamma - Y_2Si_2O_7$	(1671) <1813> {1733}	(23.6) <40.6> {25.1}	(24.3) <19.9> {24.2}
Cri + Tri + Mul	(1744) <1744> {1744}	(15.0) <12.2> {24.8}	(72.8) <80.9> {51.5}
Cri + Tri + $\gamma - Y_2Si_2O_7$	(1744) <1744> {1744}	(10.4) <14.7> {15.3}	(55.4) <55.4> {49.5}
Cri + δ + $\gamma - Y_2Si_2O_7$	(1854) <1854> {1854}	(4.8) <8.0> {9.7}	(51.1) <48.8> {49.8}
Y_2SiO_5 + δ + $\gamma - Y_2Si_2O_7$	(1854) <1854> {1854}	(12.2) <35.2> {16.8}	(26.9) <21.2> {27.3}

Data in ( ) and < > are calculated according to the dataset 1 and dataset 2 after Ref 32 in the present work, respectively. Those in { } are calculated in this study

(a) Experimental data from Ref 70

(b) Experimental data from Ref 71

descriptions of the Al-Y and Y-Si have been published by Liu et al.[42] and Shukla et al.[43] respectively. The calculated phase diagram of Al-Y system and thermodynamic properties in work of Liu et al.[42] reproduces available experimental data with the same uncertainty as updated description of Lukas.[39] The results obtained with both descriptions are very similar to each other and therefore SGTE recommendation was accepted. It should be mentioned that the description of Shukla et al.[43] for Y-Si system can not be directly used in present study because different thermodynamic model (quasi-chemical) was used there.

Thermodynamic data from the Al_2O_3-SiO_2 quasibinary system were accepted from work of Dumitrescu and Sundman.[31]

The liquid phase is described by the partially ionic sublattice model, presented by a formula (Al^{3+}, Si^{4+}, Y^{3+})$_P$(O^{2-}, $SiO_4{}^{4-}$, Va, $AlO_{3/2}$, SiO_2, C)$_Q$. The Gibbs energy is expressed by equation:

$$G_M = \sum_C \sum_A y_C y_A {}^oG_{C:A} + Q y_{Va} \sum_C y_C {}^oG_C + Q \sum_N y_N {}^oG_N + RT\left[P\sum_C y_C \ln(y_C) + Q\left(\sum_A y_A \ln(y_A) + y_{Va}\ln(y_{Va}) + \sum_N y_N \ln(y_N)\right)\right] + {}^EG_M \quad \text{(Eq 1)}$$

where P and Q are stoichiometric factors changing with composition. The subscripts C, A, Va, and N denote cations, anions, vacancies, and neutral species respectively, and y_i is the site fraction of species i on a given sublattice. ${}^EG_M$ is the excess Gibbs energy derived from binary and higher order interactions. The stoichiometric coefficients P and Q are defined as

$$Q = \sum_C v_C y_C \quad \text{(Eq 2)}$$

$$P = \sum_A (-v_A) y_A + Q y_{Va} \quad \text{(Eq 3)}$$

where v_i is the charge on species i.

Vacancies were included in the anionic sub-lattice as well as carbon to describe metallic liquid. It should be mentioned that in some sub systems, like Al-O, the liquid phase has a wide miscibility gap separating metallic and oxide liquids, while in the other systems, i.e. in the Y-O binary system, there is no miscibility gap. Therefore it is important to have a single phase description for liquid to cover these different cases.

Except for the mullite and YAM (monoclinic yttrium aluminate phase, $Y_4Al_2O_9$) phases, all the solid phases in the Y_2O_3-Al_2O_3-SiO_2 ternary system are treated as stoichiometric compounds. Four modifications (α, β, γ, δ) of $Y_2Si_2O_7$ phase were considered. For the Y_2SiO_5 only the B modification is considered due to lack of data for the A modification. Two yttria modifications, Y_2O_3-R (cubic C-type) and Y_2O_3-H (hexagonal), are considered and narrow homogeneity ranges in these phases were modelled by sublattice model. Three modifications of silica cristobalite, tridymite and quartz were described as stoichiometric compounds. The homogeneity range in mullite phase and SiO_2 solubility in the YAM phase were modelled by a sublattice model in the form of compound energy formalism.[44] The Gibbs energy of these phases is given by:

$$G_M = \sum_J \Delta_f {}^oG_{end} \Pi y_J^S + RT \sum_S \sum_J n^S y_J^S \ln(y_J^S) + {}^EG_M \quad \text{(Eq 4)}$$

where S and J denote the sublattice and species, respectively, and ${}^oG_{end}$ is the Gibbs energy of the end members.

The sublattice model was also used to describe homogeneity ranges in several phases in the Al-C-O-Si-Y system. Terminal solutions fcc, bcc, hcp and diamond were described by a two sublattice model. Solubility of Si in the Al_4C phase, solubility of O and C in the Y_5Si_3 phase, homogeneity range in the Y_2C_3 phase in the Y-C system, homogeneity range in the γ-phase in the Y-C binary and solubility of O in γ-phase were also modelled by a sublattice model.[33]

4. Thermodynamic Optimizations

For the optimization of thermodynamic parameters and calculation of phase diagrams, the THERMO-CALC program package was used.[45] Thermodynamic parameters assessed by this work are listed in Table 2.

Table 2 Thermodynamic parameters assessed by this work

Liquid (Al^{3+}, Si^{4+}, Y^{3+})$_P$(O^{2-}, $SiO_4{}^{4-}$, Va, $AlO_{3/2}$, SiO_2, C)$_Q$		
Y^{3+}(O^{2-},Va)	L^0	238524 − 134.7162 * T
Y^{3+}(O^{2-},SiO_2)	L^0	84910 − 101.2572 * T
Y^{3+}(O^{2-},SiO_2)	L^1	−570136 + 178.1970 * T
Y^{3+}(O^{2-},$SiO_4{}^{4-}$,$AlO_{3/2}$)	L^0	−2412716
Y^{3+}($SiO_4{}^{4-}$,$AlO_{3/2}$)	L^0	848816 + 54.60616 * T
Y^{3+}($SiO_4{}^{4-}$,$AlO_{3/2}$)	L^1	524377
Y^{3+}($SIO_4{}^{4-}$,$AlO_{3/2}$,SiO_2)	L^0	−2976431
Bcc (Si,Y) (C,O,Va)$_3$		
Y:O	L^0	−158000 + 114.1952 * T
Y(O,Va)	L^0	−2342689 + 98.2777 * T
Y(O,Va)	L^1	−764174
Hcp (Al,Si,Y)(C,O,Va)		
Y:O	L^0	−592135 + 73.5098 * T
Y(O,Va)	L^0	3500
Gamma Y(C,C_2,O,Va)		
Y(C,O)	L^0	−200000
Y(C,O)	L^1	100000
YAM (Al^{3+},Si^{4+})$_2$(Y^{3+})$_4$(O^{2-},Va)(O^{2-})$_9$		
(Al^{3+},Si^{4+})$Y^{3+}O^{2-}O^{2-}$	L^0	760241 + 9.998 * T
$Al^{3+}Y^{3+}$(O^{2-},Va)O^{2-}	L^0	−336375 + 132.586 * T
$Si^{4+}Y^{3+}$(O^{2-},Va)O^{2-}	L^0	−417660 − 258.293 * T
(Al^{3+},Si^{4+})Y^{3+}VaO^{2-}	L^0	−236373 + 122.137 * T
γ−$Y_2Si_2O_7$		
$Y_2Si_2O_7$	G^0	−3925077 + 1591.0739 * T −264.23561 * T * ln$T$ − 0.0129019088 * T^2 +3559383/T
Y_2SiO_5		
Y_2SiO_5	G^0	−2963134 + 1057.602 * T −181.294814 * T * ln$T$ −0.0110113475 * T^2 + 1803501/T

4.1 Y-O Binary System

The Y-O binary system was re-optimized in this work. For the optimization, phase diagram data and thermo-chemical properties of the different phases of the system were used. The Y-O system contains the following phases: α-yttrium, β-yttrium, Y_2O_3-R, Y_2O_3-H, Y-O liquid, and gas. α-Yttrium (hcp structure) is stable up to 1751 K, where it transforms into β-yttrium (bcc structure). β-Yttrium melts at 1795 K. Both α-Y and β-Y can dissolve considerable amounts of oxygen in their structure. Thermodynamic evaluations of the Y-O system have been published by Gröbner,[33] Ran et al.,[46] Lysenko[47] and Swamy et al.[48] All four evaluations have used essentially the same thermodynamic models to describe the condensed solution phases; those originally adopted by Ran et al.,[46] while they differ with regard to the experimental data used. The solubility of oxygen in α- and β-yttrium modifications was described as

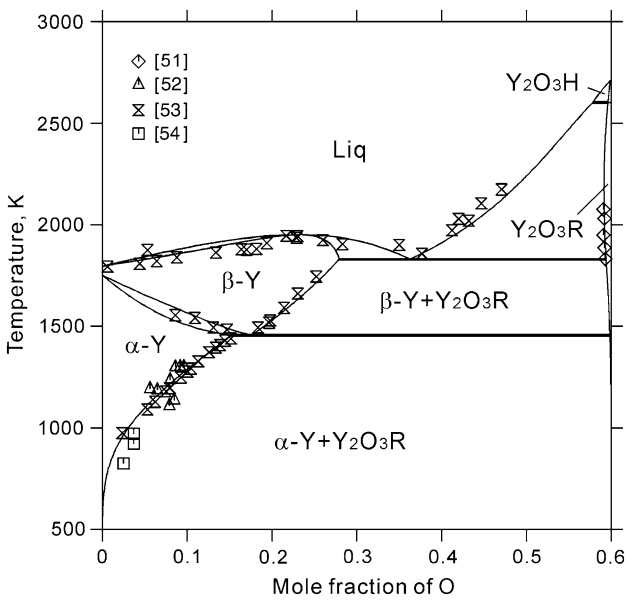

Fig. 1 The calculated Y-O phase diagram compared with experimental data

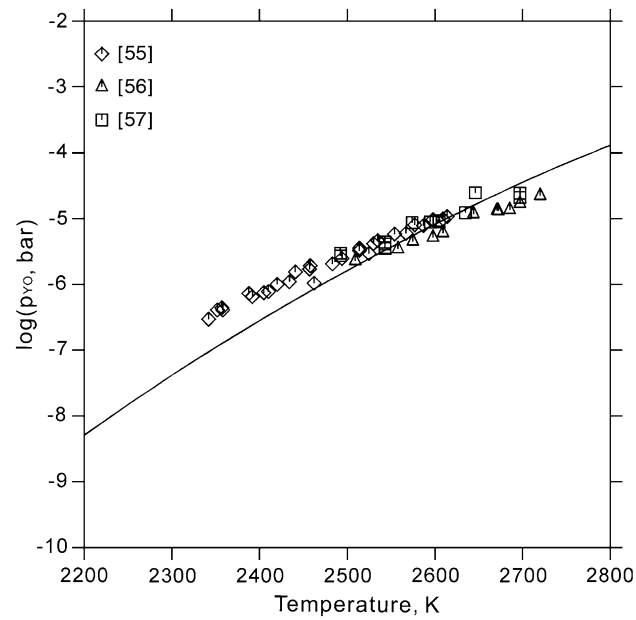

Fig. 3 The calculated equilibrium YO (g) pressures over Y_2O_3 compared with experimental data

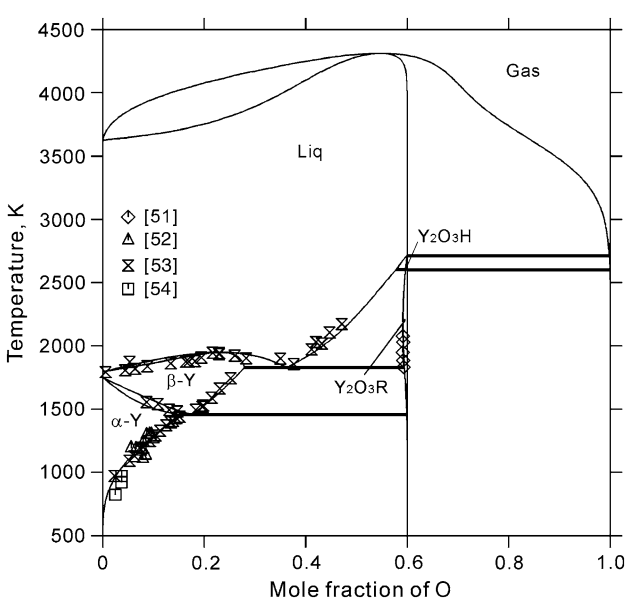

Fig. 2 The calculated Y-O phase diagram up to high temperatures

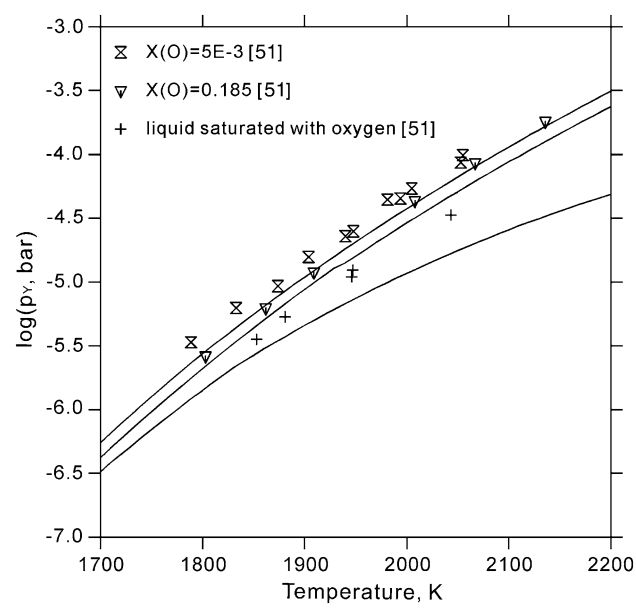

Fig. 4 The calculated equilibrium yttrium pressures over the liquid compared with experimental data

interstitial solution by sublattice model. The Wagner-Schottky model in the form of sublattice model was used to describe the small deviation from the stoichiometry of α-yttria (Y_2O_3-R) and the same model was applied to the high-temperature polymorph, β-yttria (Y_2O_3-H). Recently new assessment of Djurovic et al.[49] has been published. They used a model for bcc phase which was different from SGTE recommendation. Their model of Y_2O_3 phases was selected to make it consistent with ZrO_2-Y_2O_3 description. The existence of Y^{2+} ions assumed by Djurovic et al.[49] is experimentally not established. In the present study, the phase models were selected the same as in work of Swamy et al.[48] Thermodynamic parameters of the Y_2O_3 modifications were accepted from Zinkevich.[50]

Calculated Y-O binary phase diagrams are shown in Fig. 1 along with experimental data.[51-54] The experimental solvus, solidus, and liquidus relations are very well reproduced by calculation. Also, the calculated eutectoid and eutectic reactions are consistent with the experimental data. Special care was taken in the Y-rich side at high temperature, because if description of Swamy et al.[48] is used in combination with gas description from SGTE (SSUB database) the Y_2O_3_H phase will appear stable at high temperatures in the Y-rich composition range according to calculations. As shown in Fig. 2, the present thermodynamic data set gives reasonable predictions at temperatures above 3500 K, and thus, adequately describes the phase relations in the Y-O system in wide range of temperatures and compositions.

Thermodynamic data[51,52,55-57] were also considered in this optimization. The vapor pressure of yttrium monoxide over a solid yttrium sesquioxide and the calculated vapor

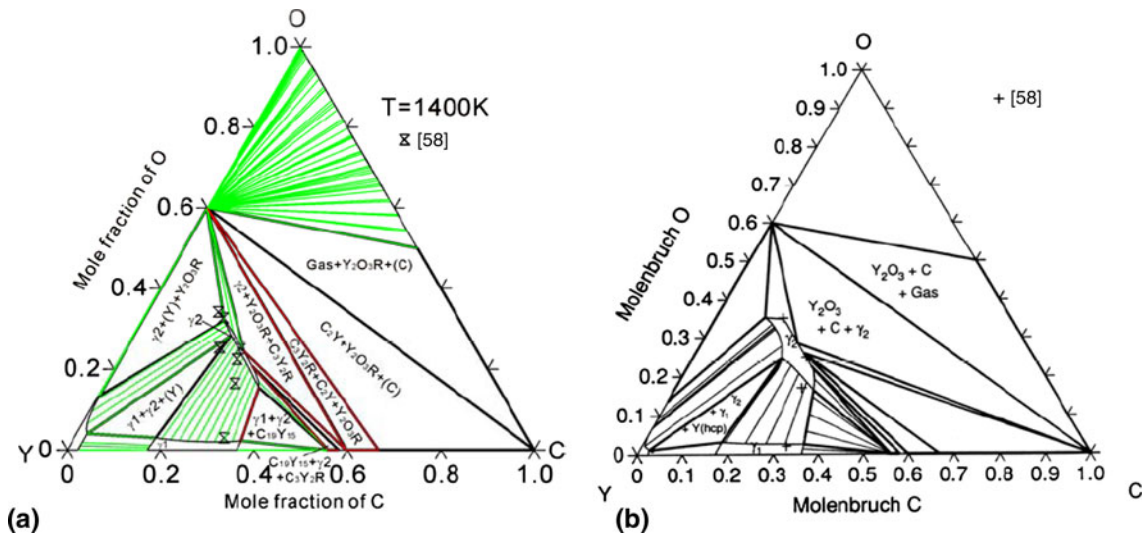

Fig. 5 Calculated isothermal section of Y-C-O ternary system at 1400 K along with experimental data[58]; (a) this work and (b) Ref 33

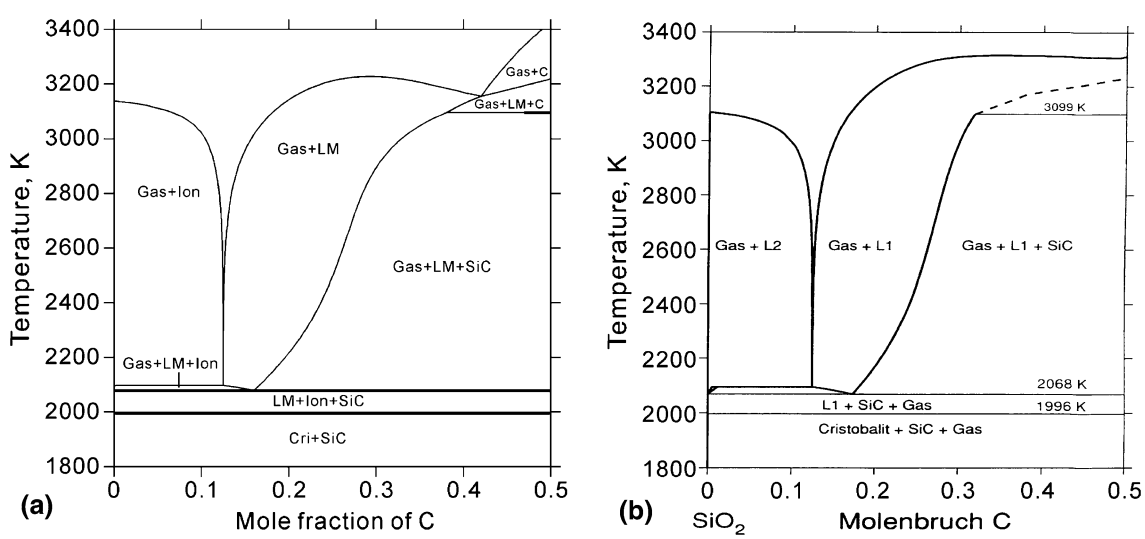

Fig. 6 Calculated SiO_2-SiC vertical section in Si-C-O ternary system: (a) this work and (b) Ref 33

pressure of yttrium over the liquid containing unsaturating and saturating amounts of sesquioxide were calculated and compared with experimental data[51,52,55-57] (Fig. 3 and 4, respectively). The present calculations reproduce experimental data within uncertainty of measurements.

4.2 Ternary Systems

Nine ternary systems, Al-C-Si, Al-C-O, Al-C-Y, Al-O-Y, Al-Si-Y, C-Si-Y, C-O-Si, C-Y-O and O-Si-Y, were recalculated and compared with previous work of Gröbner.[33] The change of data for Y caused changes in the ternary system Y-O-C, namely the homogeneity range of gamma (γ_2) phase became very narrow thus conflicting with the experimental data of Brozek et al.[58] Ternary parameters of gamma phase in the Y-O-C system were adjusted to satisfy experimental data[58] (Fig. 5). It should be mentioned that tie-lines between Y_2O_3, γ_2, C, C_2Y_3, and C_2Y phases calculated with present description are in agreement with experimental results[58] contrary to previous description of Gröbner.[33]

Several differences in ternary phase diagrams calculated using the present description and in work of Gröbner[33] can be explained by calculation problems arising due to the use of the older TC version by Gröbner.[33] For example, from a

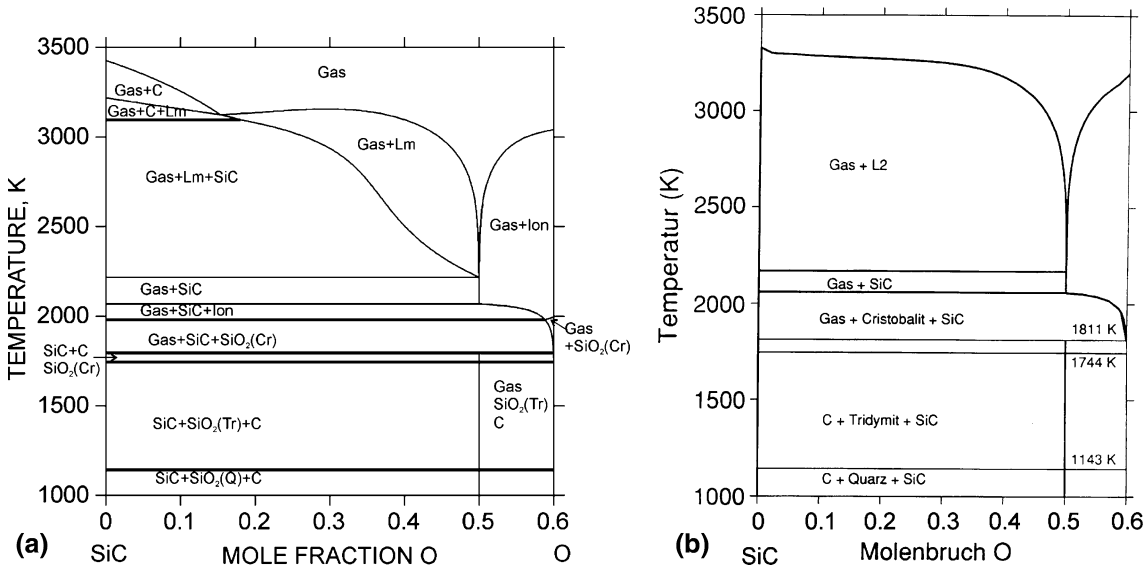

Fig. 7 Calculated section SiC-O: (a) present work and (b) Ref 33

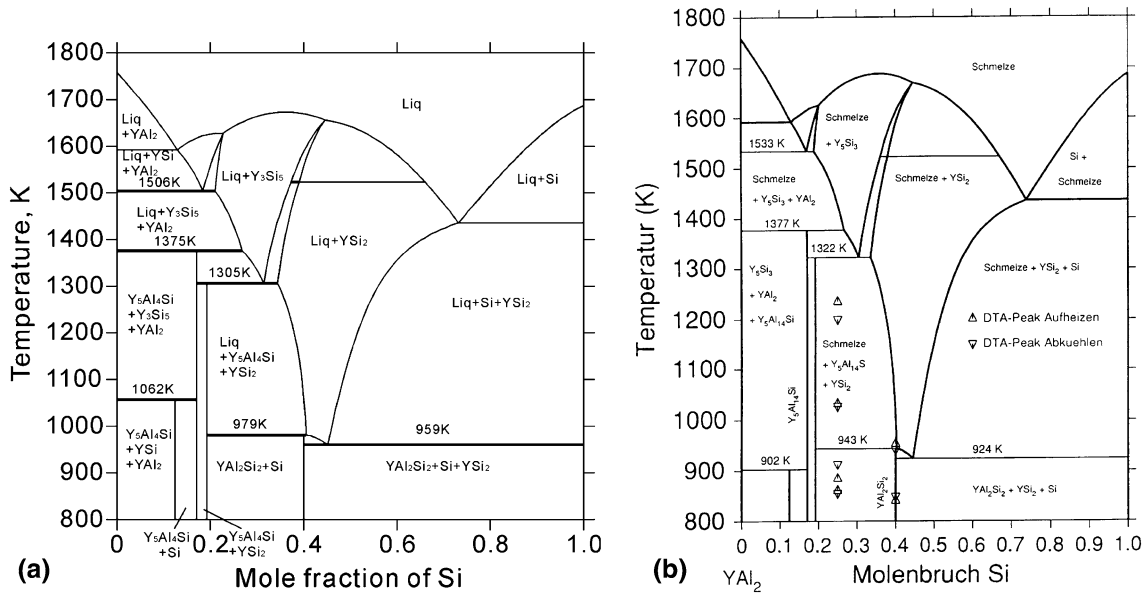

Fig. 8 Calculated section YAl_2-Si: (a) present work and (b) Ref 33

comparison of the SiO_2-SiC isopleths of the Si-C-O system presented in Fig. 6(a) with the work of Gröbner[33] (Fig. 6b) it can be concluded that problems at high temperature are now resolved. Another example for the SiC-O isopleths can be found in Fig. 7(a) and (b).

Some temperatures of invariant equilibrium changed because parameters of binary compounds in binary systems were changed. For example, in the YAl_2-Si vertical section of Y-Al-Si ternary system presented in Fig. 8(a) and (b), temperature of the heterogeneous reaction $Y_3Si_5 + YAl_2 = Y_5Al_{14}Si + YSi$ is 1062 K according to calculations based on the present thermodynamic description and 902 K calculated by Gröbner.[33] In the same vertical section, difference in calculated temperatures between present work and Gröbner's[33] (shown in brackets, respectively) was indicated for several reactions, i.e. $Liq + YSi = Y_3Si_5 + YAl_2$ (1506 and 1533 K), $YAl_2Si_2 = L + YSi_2$ (979 and 943 K) and others. However, there are no experimental data for these invariant reactions and therefore parameters for the $Y_5Al_{14}Si$, YAl_2Si_2 phases or liquid were not re-optimized.

4.3 The Y_2O_3-Al_2O_3-SiO_2 System

Thermodynamic description of Y_2O_3-Al_2O_3 binary system was taken from Fabrichnaya et al.[59] The thermodynamic parameters for the liquid phase in the Y_2O_3-SiO_2 ternary system was re-optimized in present work. The calculated phase diagram is shown in Fig. 9 along with experimental data.[60-69] Thermodynamic parameters for the YAM and liquid phases in the Y_2O_3-Al_2O_3-SiO_2 ternary system were re-optimized using experimental data [70,71] and phase diagrams were recalculated. Liquidus surface calculated with the new description is presented in Fig. 10. The temperatures and liquid compositions of invariant reactions calculated with the new description are presented in comparison with experimental data and calculations of Mao et al.[30] in Table 1.

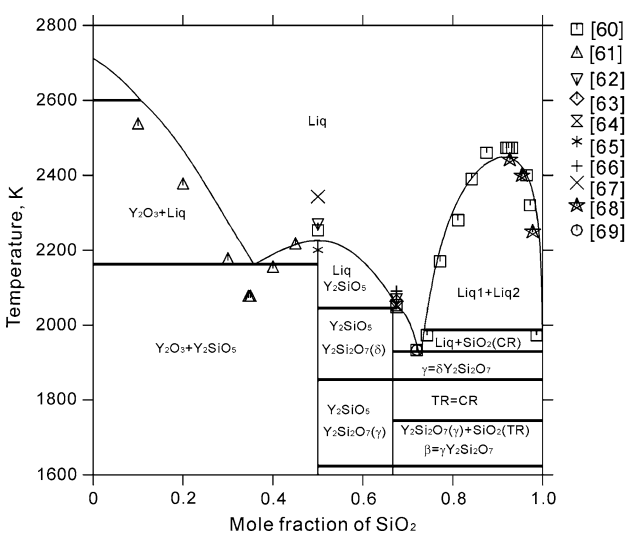

Fig. 9 Calculated phase diagram of the Y_2O_3-SiO_2 system

4.4 SiC-Y_2O_3-Al_2O_3-SiO_2 System

4.4.1 Y_2O_3-SiC. To investigate the effect of carbon content on phase equilibria, the Y_2O_3-Si-C section in the Si-C-Y-O system was calculated at 2173 K (Fig. 11). Gas was always found to be in equilibrium with the condensed phases when 0.01 mole fraction of Ar was appended to the system. No ionic liquid was found stable at 2173 K in present calculations, because the temperature is much below the melting point of Y_2O_3. According to calculations, liquid metal forms when the carbon content is less than that along the SiC-Y_2O_3 line, while at higher carbon contents, gamma and graphite phases form.

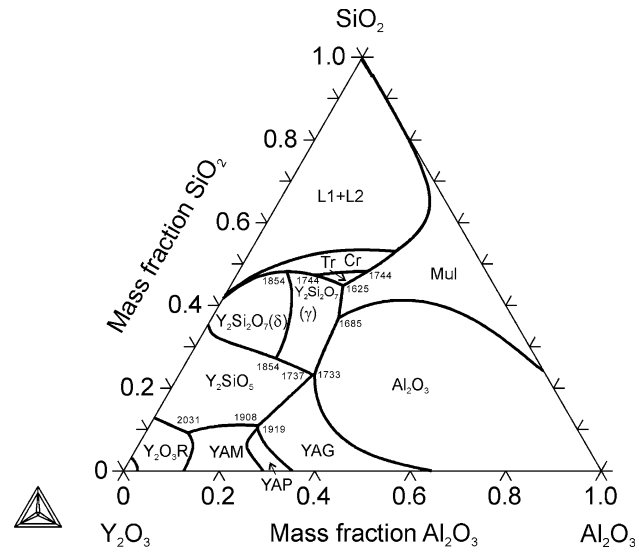

Fig. 10 The calculated liquidus surface of the Al_2O_3-Y_2O_3-SiO_2 system; unit of temperature in this phase diagram is K

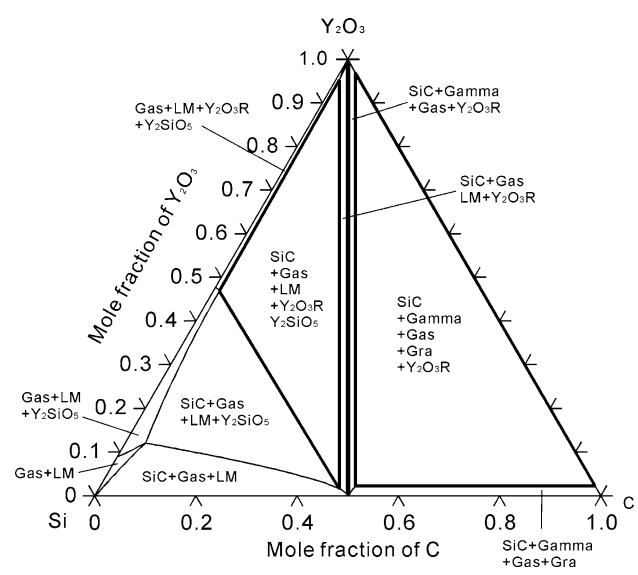

Fig. 11 Calculated isothermal section of the Si-C-Y_2O_3 system at 2173 K

These calculations show that the expected compositions strongly depend on the carbon activity. This is in agreement with previous experimental results.[22]

4.4.2 SiC-Y_2O_3-Al_2O_3-SiO_2. Using the dataset re-assessed in this work, influence of Al_2O_3 and Y_2O_3 as additives in SiC liquid phase sintering was investigated by calculations and compared with experimental data. Since SiO_2 is always present as a surface layer on the SiC powder, the system as SiC-Y_2O_3-Al_2O_3-SiO_2 was considered. Taking into account that most of the SiO_2 decomposes during sintering[72] the calculation of the SiO_2 free composition is also important.

The calculations were carried out without consideration of SiC solubility in the liquid phase.

According to calculations both the CO and SiO-partial pressures were highest in materials with large content of SiO_2, which is consistent with work of Can et al.[72]

The calculated amount of the liquid phase formed for different Al_2O_3/Y_2O_3 ratios and SiO_2 content at temperatures of 1600 and 1925 °C are presented in Fig. 12(a) and (b). Calculations at 1600 °C show the amount of liquid to have a maximum at $Al_2O_3/Y_2O_3 = 1$ for the high SiO_2 content. It strongly decreases with decreasing SiO_2 content for all Al_2O_3/Y_2O_3 ratios. For the $Al_2O_3/Y_2O_3 = 0.5$ and SiO_2 content 1% and below no liquid forms according to calculations. Calculations at 1925 °C show a slight increase of liquid amount with increase of SiO_2 content and practically no dependence on the Al_2O_3/Y_2O_3 ratio.

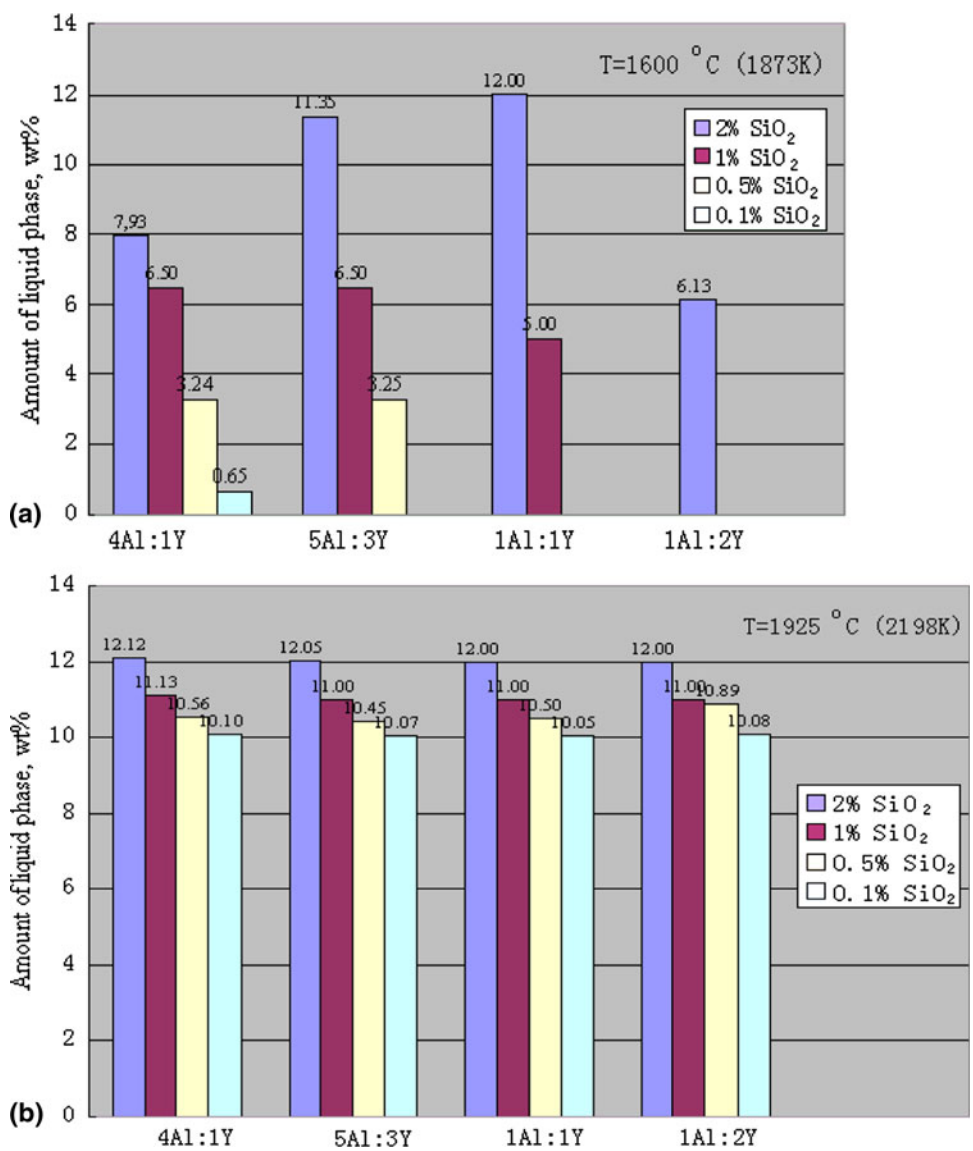

Fig. 12 Calculated amount of liquid phase in a material with 10 wt.% additives depending on the Al_2O_3/Y_2O_3 additive mole ratio at 1600 °C (a) and 1925 °C (b) for different SiO_2 contents (amount in wt.%) in the additives

The phase relations in the sub-solidus region at 1400 °C (1673 K) calculated using the database derived in present study in absence of free oxygen and SiO_2 are compared with experimental results obtained by XRD investigation of annealed samples[73] in Table 3. The calculated results are in good agreement with the experimental data. Small amounts of the YAM phase (in samples YAlSiC-455510 and YAlSiC-455520) found in experiments are probably kinetically determined. Very small amounts of Al_4SiC_4 (<0.34 wt.%) indicated by calculations for samples YAlSiC-604010, YAlSiC-604020, YAlSiC-802010 and YAlSiC-802050 were not detected experimentally in the microstructure nor by XRD. The reason of these small deviations is the reaction of SiC with YAM and Al_2O_3 resulting in dissolution of the SiO_2 in YAM and formation of the Al_4SiC_4 phase. The calculated isothermal section of the SiC-Y_2O_3-Al_2O_3 system is presented in Fig. 13. It should be mentioned that graphite phase forms in the Y_2O_3-rich composition range in a very small amount ($\sim 10^{-5}$-10^{-4} wt.%) and therefore this information is not presented in Table 3. Phase relations were also calculated at high temperature (1850/1950 °C). The phase composition was in good agreement with the calculated data.

Temperatures of melting of the same compositions as in Table 3 were calculated assuming that the system does not contain SiO_2. Comparison of melting temperatures of the same samples determined experimentally with calculated results (see Fig. 14) indicated reasonably good agreement in the Al_2O_3-rich compositions, while for the Y_2O_3 rich compositions melting temperatures determined by STA (simultaneous thermal analysis) in Ref 67 are up to ~75 °C higher than obtained by calculation of phase equilibrium. The melting according to present calculations are accompanied by formation and dissolution of SiO_2 and a small amount of C in liquid phase as well as formation of Al_4SiC_4, and γ-phase depending on the composition. Metal liquid is indicated to form in all calculated mixtures. Formation of additional phases (Al_4SiC_4 and γ-phases) depended only on Y_2O_3/Al_2O_3 ratio but not on SiC content. Al_4SiC_4 phase did not form in Al_2O_3-rich compositions. According to

Table 3 Phase composition after preparation in SPS at 1400 °C (comparison between XRD and calculated results)

Sample/composition (mol%)Y_2O_3 Al_2O_3 SiC	SiC, wt.%	Al_2O_3, wt.%	YAG, wt.%	YAP, wt.%	YAM, wt.%	Y_2O_3, wt.%	Al_4SiC_4, wt.%	Residual Rwp, %
YAlSiC-208010								
18 72 10								
Experimental	3.8	38.6	57.7					6.5
Thermodyn. calculation	3.4	36.3	60.3					
YAlSiC-208020								
16 64 20								
Experimental	9	36.0	55.1					6.8
Thermodyn. calculation	7.3	34.8	57.9					
YAlSiC-455510								
40.5 49.5 10								
Experimental	2.5		35.4	57.2	4.9			6.1
Thermodyn. calculation	2.7		36.6	60.6				
YAlSiC-455520								
36 44 20								
Experimental	5.7		38.2	51.6	4.5			5.7
Thermodyn. calculation	6.0		35.4	58.6				
YAlSiC-604010								
54 36 10								
Experimental	1.9			42.5	55.7			6.1
Thermodyn. calculation	2.17			35.66	61.83		0.34	
YAlSiC-604020								
48 32 20								
Experimental	4.6			43.0	52.4			6.1
Thermodyn. calculation	5.09			34.60	59.98		0.33	
YAlSiC-802010								
72 18 10								
Experimental	3.5				52.6	44.0		7.3
Thermodyn. calculation	1.95				53.54	44.26	0.25	
YAlSiC-802050								
40 10 50								
Experimental	15.7				50.2	34.1		6.7
Thermodyn. calculation	16.44				45.63	37.72	0.21	

calculation, formation of Al_4SiC_4 occurred for ratios of Y_2O_3/Al_2O_3 equal to 45/55 and 60/40, in Y_2O_3-rich composition, γ-phase was forming. This interaction was not observed experimentally and could be the reason for the differences. The absence of experimental evidences for the interaction could be caused by kinetic reasons. The interaction is very slow or the formation of SiO_2 could have a lower rate than the rate of evaporation of SiO_2. It should be mentioned that melting temperatures calculated in this study for SiC-free samples were ~20 °C lower than those determined in experiments.[73] This difference is quite acceptable taking into account higher uncertainty of experimental data used in optimization of the Al_2O_3-Y_2O_3 system.[59] An additional reason for inconsistency could be that the thermodynamic model of the liquid does not include species of SiC. A next step for further improving of the thermodynamic model would be the introduction of SiC as neutral species in the model of liquid.

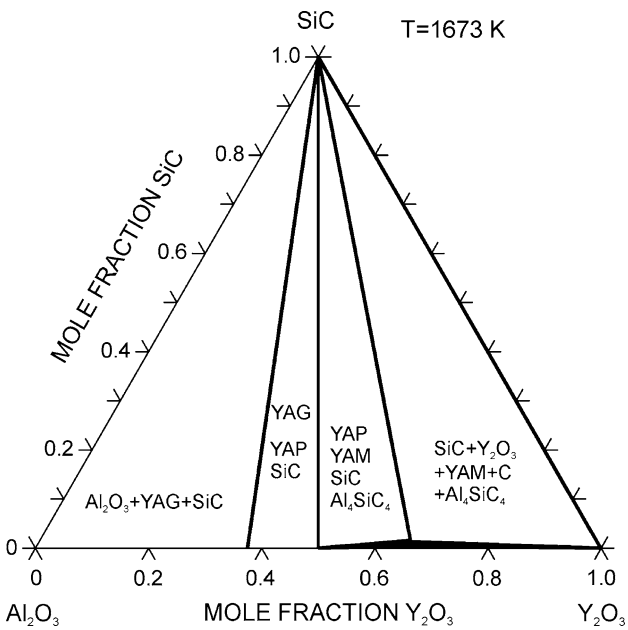

Fig. 13 Calculated isothermal section the SiC-Al_2O_3-Y_2O_3 system at 1400 °C

5. Conclusion

Taking into account the new description of yttrium, the database for the Si-C-Al-Y-O system was completely revised. The Y-O binary system was re-optimized in this work. For the optimization, phase diagram data and thermochemical properties of the different phases of the system were used. The parameters of the liquid phase in the Y_2O_3-SiO_2 system were re-optimized in this work. In ternary system Al_2O_3-Y_2O_3-SiO_2, mixing parameters of YAM phase and ternary mixing parameters of liquid phase were re-optimized. Phase diagrams of Al_2O_3-Y_2O_3-SiO_2, and SiC-Y_2O_3-SiO_2 systems were re-calculated and compared with earlier works. Phase diagram of the SiC-Al_2O_3-Y_2O_3 systems was calculated at 1400 °C using updated description. Influence of SiO_2 content and Al_2O_3/Y_2O_3 ratio on amount of liquid forming at 1600 and 1925 °C was investigated using computational thermodynamics. Phase amounts calculated using an updated thermodynamic description of the SiC-Al_2O_3-Y_2O_3 system indicated good agreement with experimentally studied compositions. However, comparison of melting temperatures of the same samples studied experimentally with calculated results reveals lower temperature of melting especially for the Y_2O_3 rich compositions.

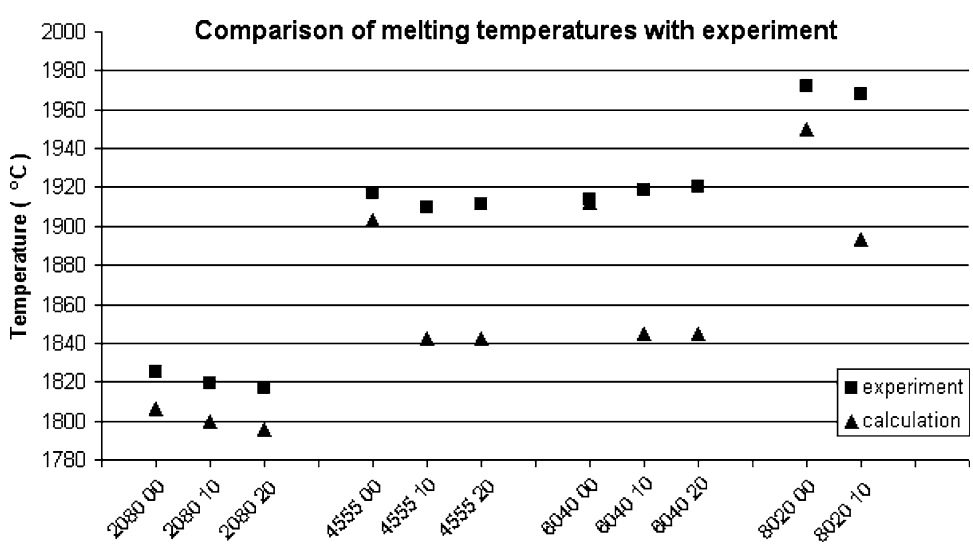

Fig. 14 Comparison of melting temperatures determined experimentally in work of Ref 73 with calculations performed in the present study

Acknowledgment

This work was supported by the German Research Foundation contract SE 647/10-1 and HE 2457/14-2.

References

1. M. Omori and H. Takei, Pressureless Sintering of SiC, *J. Am. Ceram. Soc.*, 1982, **65**(6), p C-92
2. K.A. Schwetz, SiC Based Hard Materials, *Handbook of Ceramic Hard Materials*, 2nd ed., R. Riedel, Ed., Wiley-VCH, Weinheim, NY, 2000, p 683-748
3. V.D. Krstic, M.D. Vlajic, and R.A. Verrall, Silicon Carbide Ceramics for Nuclear Application, *Key Eng. Mater.*, 1996, **122-124**, p 387-396
4. R.A. Verrall, M.D. Vlajic, and V.D. Krstic, Silicon Carbide as an Inert-Matrix for a Thermal Reactor Fuel, *J. Nucl. Mater.*, 1999, **274**(2-3), p 54-60
5. K.H. Sarma, J. Fourcade, S.G. Lee, and A.A. Solomon, New Processing Methods to Produce Silicon Carbide and Beryllium Oxide Inert Matrix and Enhanced Thermal Conductivity Oxide Fuels, *J. Nucl. Mater.*, 2006, **352**(1-3), p 324-333
6. Z. Pan, H.J. Seifert, O. Fabrichnaya, R. Baney, and J. Tulenko, Phase Reactions of Ceria in LPS SiC, *High Temperature Corrosion and Materials Chemistry 7*, Vol 16(44), E. Wuchina, E. Opila, J. Fergus, T. Maruyama, and D. Shifler, Ed., 214th ECS Meeting, October 12-17, 2008, Honolulu, HI, p 65-80
7. L.S. Sigl and H.J. Kleebe, Core/Rim Structure of Liquid-Phase-Sintered Silicon Carbide, *J. Am. Ceram. Soc.*, 1993, **76**(3), p 773-776
8. N.P. Padture, In Situ-Toughened Silicon Carbide, *J. Am. Ceram. Soc.*, 1994, **77**(2), p 519-523
9. J.K. Lee, H. Tanaka, and H. Kim, Movement of Liquid Phase and the Formation of Surface Reaction Layer on the Sintering of β-SiC with an Additive of Yttrium Aluminium Garnet, *J. Mater. Sci. Lett.*, 1996, **15**(5), p 409-411
10. J.Y. Kim and Y.W. Kim, Microstructure and Mechanical Properties of α-Silicon Carbide Sintered with Yttrium-Aluminum Garnet and Silica, *Commun. Am. Ceram. Soc.*, 1999, **82**(2), p 441-444
11. A.K. Samanta, K.K. Dhargupta, and S. Ghatak, Decomposition Reactions in the SiC–Al–Y–O System During Gas Pressure Sintering, *Ceram. Int.*, 2001, **27**(2), p 123-133
12. H.W. Xu, T. Bhatia, and A. Swarnima, Microstructural Evolution in Liquid-Phase-Sintered SiC: Part I, Effect of Starting Powder, *J. Am. Ceram. Soc.*, 2001, **84**(7), p 1578-1584
13. L. Gao, H.Z. Wang, H. Kawaoka, T. Sekino, and K. Niihara, Fabrication of YAG–SiC Nanocomposites by Spark Plasma Sintering, *J. Eur. Ceram. Soc.*, 2002, **22**(5), p 785-789
14. J.W. Wang, H. Yang, and X.Z. Guo, Preparation of SiC-$Y_3Al_5O_{12}$ Composite Ceramics by Adding Sintering Aids via Sol-Gel Method, *J. Refract. Mater.*, 2005, **39**(3), p 192-195
15. O. Borrero-López, A.L. Ortiz, F. Guiberteau, and P. Padture, Effect of Liquid-Phase Content on the Contact-Mechanical Properties of Liquid-Phase-Sintered α-SiC, *J. Eur. Ceram. Soc.*, 2007, **27**(6), p 2521-2527
16. T. Grande, H. Sommerset, E. Hagen, K. Wilk, and M.A. Einarsrud, Effect of Weight Loss on Liquid-Phase-Sintered Silicon Carbide, *J. Am. Ceram. Soc.*, 1997, **80**(4), p 1047-1052
17. M.A. Mulla and V.D. Krstic, Low-Temperature Pressureless Sintering of Beta-Silicon Carbide with Aluminum Oxide and Yttrium Oxide Additions, *Am. Ceram. Soc. Bull.*, 1991, **70**(3), p 439-441
18. Y.W. Kim, M. Mitomo, and J.G. Lee, Influence of Silica Content on Liquid Phase Sintering of Silicon Carbide with Yttrium-Aluminum Garnet, *J. Ceram. Soc. Jpn.*, 1996, **104**(9), p 816-818
19. F.K. van Dijen and E. Mayer, Liquid Phase Sintering of Silicon Carbide, *J. Eur. Ceram. Soc.*, 1996, **16**(4), p 413-420
20. F.K.L. Falk, Microstructural Development During Liquid Phase Sintering of Silicon Carbide Ceramics, *J. Eur. Ceram. Soc.*, 1997, **17**(8), p 983-994
21. W.J. Clegg, Role of Carbon in the Sintering of Boron-Doped Silicon Carbide, *J. Am. Ceram. Soc.*, 2000, **83**(5), p 1039-1043
22. J. Ihle, M. Herrmann, and J. Adle, Phase Formation in Porous Liquid Phase Sintered Silicon Carbide, Part I–IIII, *J. Eur. Ceram. Soc.*, 2005, **25**(7), p 987-1013
23. T. Grande, H. Sommerset, E. Hagen, K. Wiik, and M.-A. Einarsrud, Effect of Weight Loss on Liquid-Phase-Sintered Silicon Carbide, *J. Am. Ceram. Soc.*, 1997, **80**(4), p 1047-1052
24. S. Baud, F. Thevenot, A. Pisch, and C. Chatillon, High Temperature Sintering of SiC with Oxide Additives: IV: Powder Beds and the Influence of Vaporization on the Behaviour of SiC Compacts, *J. Eur. Ceram. Soc.*, 2003, **23**(1), p 29-36
25. S. Baud, F. Thevenot, A. Pisch, and C. Chatillon, High Temperature Sintering of SiC with Oxide Additives: I. Analysis in the SiC-Al_2O_3 and SiC-Al_2O_3–Y_2O_3 Systems, *J. Eur. Ceram. Soc.*, 2003, **23**(1), p 1-8
26. A.K. Misra, Thermochemical Analysis of the Silicon-Carbide-Alumina Reaction with Reference to Liquid Phase Sintering of Silicon Carbide, *J. Am. Ceram. Soc.*, 1991, **74**(2), p 345-351
27. M.A. Mulla, V.D. Krstic, and W.T. Thompson, Reaction-Inhibition During Sintering of SiC with Al_2O_3 Additions, *Can. Metall. Quart.*, 1995, **34**(4), p 357-362
28. J.H. She and K. Ueno, Effect of Additive Content on Liquid-Phase Sintering on Silicon Carbide, *Mater. Res. Bull.*, 1999, **34**(10-11), p 1629-1636
29. O. Fabrichnaya, H.J. Seifert, R. Weiland, T. Ludwig, F. Aldinger, and A. Navrotsky, Phase Equilibria and Thermodynamics in the Y_2O_3-Al_2O_3-SiO_2 System, *Z. Metallkd.*, 2001, **92**(9), p 1083-1097
30. H. Mao, M. Selleby, and O. Fabrichnaya, Thermodynamic Reassessment of the Y_2O_3-Al_2O_3-SiO_2 System and its Subsystem, *CALPHAD*, 2008, **32**(2), p 399-412
31. L. Dumitrscu and B. Sundman, A Thermodynamic Reassessment of the SI-AL-O-N System, *J. Eur. Ceram. Soc.*, 1995, **15**(3), p 239-247
32. H. Mao and M. Selleby, Thermodynamic Reassessment of the Si_3N_4-AlN-Al_2O_3-SiO_2 System—Modeling of the SiAlON and Liquid Phases, *CALPHAD*, 2007, **31**(2), p 269-280
33. J. Gröbner, "Konstitutionsberechnungen in System Y-Al-Si-C-O," Ph.D. Thesis, University of Stuttgart, Germany, 1994
34. D.M. Cupid, O. Fabrichnaya, and H.J. Seifert, Thermodynamic Aspects of Liquid Phase Sintering of SiC Using Al_2O_3 and Y_2O_3, *Int. J. Mater. Res.*, 2007, **98**(10), p 976-986
35. Scientific Group Thermodata Europe (SGTE). http://www.SGTE.org
36. N. Saunders and P. Miodwnik, *CALPHAD (Calculation of Phase Diagram): A Comprehensive Guide*, Pergamon, Oxford, 1998
37. H.L. Lukas, S.G. Fries, and B. Sundman, *Computational Thermodynamics*, Cambridge University Press, Cambridge, 2007
38. A.T. Dinsdale, SGTE Data for Pure Elements, *CALPHAD*, 1991, **15**(4), p 317-425

39. SGTE, Al-Y, *Landolt-Börnstein Group IV: Physical Chemistry*, Vol 19, W. Martienssen, Ed., Thermodynamic Properties of Inorganic Materials Compiled by SGTE, Binary Systems Part 1, Springer, Berlin, 2002
40. SGTE, C-Y, *Landolt-Börnstein Group IV: Physical Chemistry*, Vol 19, W. Martienssen, Ed., Thermodynamic Properties of Inorganic Materials Compiled by SGTE, Binary Systems Part 2, Springer, Berlin, 2004
41. SGTE, Si-Y, *Landolt-Börnstein Group IV: Physical Chemistry*, Vol 19, W. Martienssen, Ed., Thermodynamic Properties of Inorganic Materials Compiled by SGTE, Binary Systems Part 4, Springer, Berlin, 2006
42. S.H. Liu, Y. Du, and H.L. Chen, A Thermodynamic Reassessment of the Al-Y System, *CALPHAD*, 2006, **30**, p 334-340
43. A. Shukla, K. Youn-Bae, and A.D. Pelton, Thermodynamic Assessment of the Ce-Si, Y-Si, Mg-Ce- Si and Mg-Y-Si Systems, *Int. J. Mater. Res.*, 2009, **100**(2), p 208-217
44. M. Hillert, The Compound Energy Formalism, *J. Alloys Compd.*, 2001, **320**(2), p 161-176
45. J.O. Andresson, T. Helander, L. Höglund, P. Shi, and B. Sundman, The Thermo-Calc & Dictra, Computational Tools for Materials Science, *CALPHAD*, 2002, **26**(2), p 273-312
46. Q. Ran, H.L. Lukas, E.-T. Henig, G. Effenberg, and G. Petzow, Optimization and Calculation of the Y-O System, *Z. Metallkd.*, 1989, **80**, p 800-805
47. V.A. Lysenko, Thermodynamic Calculation of the Yttrium-Oxygen Phase Diagram, *Inorg. Mater.*, 1996, **32**(4), p 392-396
48. V. Swamy, H.J. Seifert, and F. Aldinger, Thermodynamic Properties of Y_2O_3 Phases and the Yttrium-Oxygen Phase Diagram, *J. Alloys Compd.*, 1998, **269**(1-2), p 201-207
49. D. Djurovic, M. Zinkevich, and F. Aldinger, Thermodynamic Modeling of the Yttrium-Oxygen System, *CALPHAD*, 2007, **31**(4), p 560-566
50. M. Zinkevich, Thermodynamics of Rare Earth Sesquioxides, *Prog. Mater. Sci.*, 2007, **52**(4), p 597-647
51. R.J. Ackermann, E.G. Rauh, and R.R. Walters, Thermodynamic Study of the System Yttrium + Yttrium Sesquioxide A Refinement of the Vapor Pressure of Yttrium, *J. Chem. Thermodyn.*, 1970, **2**(1), p 139-149
52. T.H. Okabe, T.N. Deura, T. Oishi, K. Ono, and D.R. Sadoway, Thermodynamic Properties of Oxygen in Yttrium-Oxygen Solid Solutions, *Metall. Mater. Trans.*, 1996, **27**(5), p 841-847
53. R.C. Tucker, E.D. Gibson, and O.N. Carlson, *International Symposium on Compounds of Interest in Nuclear Reactor Technology*, J.T. Waber, P. Chiotti, and W.N. Miner, Ed., The Metallurgical Society of the American Institute of Mining, Metallurgical and Petroleum Engineers, Littleton, CO, 1964, p 315-325
54. O.N. Carlson, R.R. Lichtenberg, and J.C. Warner, Solid Solubilities of Oxygen, Carbon and Nitrogen in Yttrium, *J. Less-Common Met.*, 1974, **35**, p 275-284
55. M.B. Liu and P.G. Wahlbeck, Knudsen Effusion and Mass-Spectrometric Studies of Vaporization of Y_2O_3(S)—Dissociation Energy of YO(G), *High Temp. Sci.*, 1974, **6**, p 179-189
56. R.J. Ackermann, E.G. Rauh, and R.J. Thorn, Thermodynamic Properties of Gaseous Yttrium Monoxide. Correlation of Bonding in Group III Transition-Metal Monoxides, *J. Chem. Phys.*, 1964, **40**(3), p 883-889
57. L.L. Ames, P.N. Walsh, and D. White, Rare Earths. IV. Dissociation Energies of the Gaseous Monoxides of the Rare Earths, *J. Phys. Chem.*, 1967, **71**(8), p 2707-2718
58. V. Brozek, P. Karen, and B. Hajek, Studies of Hydrolysable Carbides XXVI: Composition Limits of the NaCl-Type Yttrium Oxycarbide Phase, *J. Less Common Met.*, 1985, **107**(2), p 295-299
59. O. Fabrichnaya, M. Zinkevich, and F. Aldinger, Thermodynamic Modelling in the ZrO_2-La_2O_3-Y_2O_3-Al_2O_3 System, *Int. J. Mater. Res.*, 2007, **98**(9), p 838-846
60. N.A. Toropov and I.A. Bondar, Silicates of Rare Earth Elements: 3. Phase Diagram of Binary System Yttrium Oxide—Silica, *Izv. Akad. Nauk. SSSR, Otd. Khim. Nauk.*, 1961, **4**, p 544-550
61. A. Bondar, Relationship of the Experimental Data and Theoretical Calculations of the Liquidus Temperatures in Simple Binary System, *Izv. Acad. Nauk SSSR, Ser. Khim.*, 1964, **11**, p 1921-1925
62. I. Warsaw and R. Roy, *Progress in the Science and Technology of the Rare Earth*, Vol 1, L. Eyring, Ed., Pergamon Press, New York, 1964, p 203-221
63. J. Felsche, Crystal Data on the Polymorphic Disilicate $Y_2Si_2O_7$, *Naturwiss.*, 1970, **57**(3), p 127-128
64. N.A. Toropov, I.F. Andreev, A.N. Sokolov, and L.N. Sanzharevskaya, Solid Solutions in the System $Y_2Si_2O_7$-$Ce_2Si_2O_7$, *Izv. Akad. Nauk, Neorg. Mater.*, 1970, **6**, p 519-523
65. G.V. Anan'eva, A.M. Korovkin, T.I. Merkulyaeva, A.M. Morozova, M.V. Petrov, I.V. Savinova, V.R. Startsev, and P.P. Feofilov, Growth of Lanthanide Oxyorthosilicate Single Crystals, and their Structural and Optical Characteristics, *Izv. Acad. Nauk SSSR, Ser. Neorg. Mater.*, 1981, **17**, p 1037-1042
66. G.V. Anan'eva, V.E. Karapetyan, A.M. Korovkin, T.I. Markulayeva, I.A. Peschanskaya, I.V. Savinova, and P.P. Feofilov, Structural Characteristics and Physical Properties of Lanthanide, Yttrium and Scandium Diortho(pyro)silicate Crystals Grown by Czochralski Method, *Izv. Acad. Nauk SSSR, Ser. Neorg. Mater.*, 1982, **18**, p 442-445
67. C.D. Brandle, A.J. Valentino, and G.W. Berstresser, Czochralski Growth of Rare-Earth Orthosilicates (Ln_2SiO_5), *J. Cryst. Growth*, 1986, **79**(1-3), p 308-315
68. V.B.M. Hageman and H.A.J. Oonk, Liquid Immiscibility in the SiO_2 + MgO, SiO_2 + SrO, SiO_2 + La_2O_3, and SiO_2 + Y_2O_3 Systems, *Phys. Chem. Glasses*, 1986, **27**(5), p 194-198
69. C.H. Drummond, W.E. Lee, W.A. Sanders, and J.D. Kiser, Crystallization and Characterization of Y_2O_3-SiO_2 Glasses, *Ceram. Eng. Sci. Proc.*, 1988, **9**(9/10), p 1343-1354
70. I.A. Bondar, F.Ya. Galakhov, Phase Equilibria in the System Y_2O_3-Al_2O_3-SiO_2, *Izv. Akad. Nauk SSSR, Otd. Khim. Nauk.*, 1964, **7**, p 1325-1326
71. U. Kolitsch, T. Ludwig, H.J. Seifert, and F. Aldinger, Phase Equilibria and Crystal Chemistry in the Y_2O_3-Al_2O_3-SiO_2 System, *J. Mater. Res.*, 1999, **14**(2), p 447-455
72. A. Can, M. Herrmann, D.S. Lachlan, I. Sigalas, and J. Adler, Densification of Liquid Phase Sintered Silicon Carbide, *J. Eur. Ceram. Soc.*, 2006, **26**(9), p 1707-1713
73. R. Neher, M. Herrmann, K. Brandt, K. Jaenicke-Roessler, Z. Pan, O. Fabrichnaya, and H.J. Seifert, Liquid Phase Formation in the System SiC-Al_2O_3-Y_2O_3, *J. Eur. Ceram. Soc.*, 2010 (submitted)